Fabrication of Electrically-Conducting Nonwoven Porous Mats of Polystyrene-Polypyrrole Core-Shell Nanofibers via Electrospinning and Vapor Phase Polymerization

Sujith Nair,[1)] Erik Hsiao, and Seong H. Kim*
Department of Chemical Engineering, The Pennsylvania State University
University Park, PA 16802

In order to understand the PPy growth kinetics, a cylindrical shrinking-core diffusion-reaction model was developed for a case where the diffusion coefficient decreased as the polymerization reaction proceeded and formed a diffusion barrier layer over the core. The observed PPy growth kinetics can be modeled with a cylindrical shrinking-core diffusion-reaction model.[1] It is expected that as the PPy layer grows thicker, it acts as a diffusion barrier and makes the monomer diffusion into the unreacted fiber core more difficult. The diffusion barrier effect would be especially large if the PPy layer is crystalline. Since the exact dependence of the monomer diffusion coefficient on the PPy layer thickness is not known, we *made a crude and simplest assumption* that the diffusion coefficient decreases linearly as the reaction front progresses into the fiber and simulated the time dependence of the polymer growth *to see if this model can qualitatively capture the physical situation.* There is no experimental evidence to support the linear dependence of the diffusion coefficient on the reaction front propagation distance. If the oxidants are completely segregated on the PS fiber surface, then the growth kinetic of PPy may be governed by the diffusion of pyrrole monomer within the oxidant layer whose thickness is unknown in the current experiment.

The diagrams in Figure S-1 represent the schematic model of the cylindrical shrinking-core diffusion-reaction and the radius dependence of the diffusion coefficient, D(r). In this model, it is assumed that the diffusion coefficient decreases linearly with radius with a slope of *A*

[1] J. M. Smith, *Chemical Engineering Kinetics*, 3rd Edition (McGraw Hill International Edition), Chap. 14, 642.

and reaches zero at a radius $r_{lim} = R–D_o/A$. Then, the differential mass balance equation can be expressed as:

$$-\frac{dN_m}{dt} = 2\pi r \cdot D(r)\frac{dC_m}{dr} \qquad (1)$$

where dN_m/dt is the monomer consumption rate at the reaction front $r_c(t)$ and dC_m/dr is the concentration gradient of monomer along the radial direction. If the concentration of the Fe^{III} oxidant is represented with C_{Ox} and assumed to be constant in the region between R_o and r_{lim}, then dN_m can be expressed as $-dN_m = -2\pi r_c \cdot C_{Ox} dr_c$.

Equation (1) can be solved by separating variables and integrating dr from R_o to $r_c(t)$ and dC_m from C_{mo} (monomer concentration at the fiber surface) to zero at $r_c(t)$ followed by integration of $dr_c(t)$ from R_o to r_s and dt from 0 to t. The integrated solution can then be plotted to show the conversion, $x_p(t) = \frac{R - r_c(t)}{R - r_{\lim}}$, as a function of reaction time for different A values. For a simplification, two characteristic terms are defined:

Growth time constant: $$\tau \equiv \frac{R_o^{\,2}}{D_o \cdot C_a} \quad \left(where\, C_a = \frac{C_{mo}}{C_{Ox}} \right) \qquad (2)$$

Growth limit radius: $$\frac{r_{\lim}}{R} \equiv 1 - \frac{D_o}{A \cdot R} \qquad (3)$$

Figure S-1 shows the simulation results for the polymerization time from 0 to 30 hours when τ = 500 and r_{lim}/R_o varying from 0.50 to 0.95. The simulation clearly shows that the polymer growth reaches the maximum amount faster as r_{lim}/R gets larger, i.e. as the diffusion coefficient, $D(r)$, drops faster as $r_c(t)$ moves inward. In other words, if the polymer growth kinetic shows a fast growth to the maximum amount, the PPy product layer is more accumulated near the surface region of the template fiber. Note that the use of non-dimensionalized r_{lim}/R term simplifies the solution; but this may oversimplify the large distribution of the fiber diameter and topographic or structural details of individual fibers. More accurate modeling should include the effects of these inhomogeneity.

This model is then used to fit the time dependence of the vapor phase polymerization kinetics observed with FTIR. The fit results are shown in Figure S-2. The PS-$FeCl_3$ data set can be fitted well with τ = 300 and r_{lim}/R = 0.75 while the PS-FeTS data fitted with τ = 500 and r_{lim}/R = 0.95. It is noteworthy that the experimental data is not fitted well with the regular shrinking-

core model with a constant diffusion coefficient, but reproduced very well with our model where the diffusion coefficient decreases as the product layer grows. This supports the formation of the PPy shell over the PS template fibers. The slight difference in τ could be due to the difference in the average template fiber diameter (Figure 2) and the difference in the PS-oxidant matrix structure (Figure 1). Using the average diameter of the template fibers shown in Figure 2, the $D_o \cdot C_a = R^2/\tau$ value of these two systems is calculated to be different by only 15% to each other. Since the concentrations of the Fe^{III} oxidant loaded into the template fiber are comparable in both cases and the vapor pressure of pyrrole monomer was constant during the polymerization, the similarity of the $D_o \cdot C_a$ value means that the initial diffusion coefficients of pyrrole in the template fibers are compatible to each other. This result makes sense since the pyrrole diffusion through amorphous polystyrene is not expected to be altered significantly by the Fe^{III} salt precipitates in the polymer. When the constant diffusion coefficient model is used, the $D_o \cdot C_a$ value for the PS-FeTs system is 20 times larger than that of the PS-$FeCl_3$ system, which is not consistent with the expectation.

The large difference in r_{lim}/R is noteworthy. The smaller r_{lim}/R means that the monomer can diffuse deeper into the template fiber. In other words, the PPy is distributed over a larger volume inside the PS template fiber with a lower spatial concentration in PS. In contrast, the larger r_{lim}/R results in a thinner PPy layer near the template fiber surface with a higher PPy concentration. In Figure 4, the PS template fiber peaks are much larger for the PS-Cl-PPy system than the PS-TS-PPy system. This FTIR observation is consistent with the broader cross-sectional distribution of PPy in PS-Cl-PPy (r_{lim}/R=0.75) than PS-TS-PPy (r_{lim}/R=0.95) implied in the shrinking-core kinetics analysis.

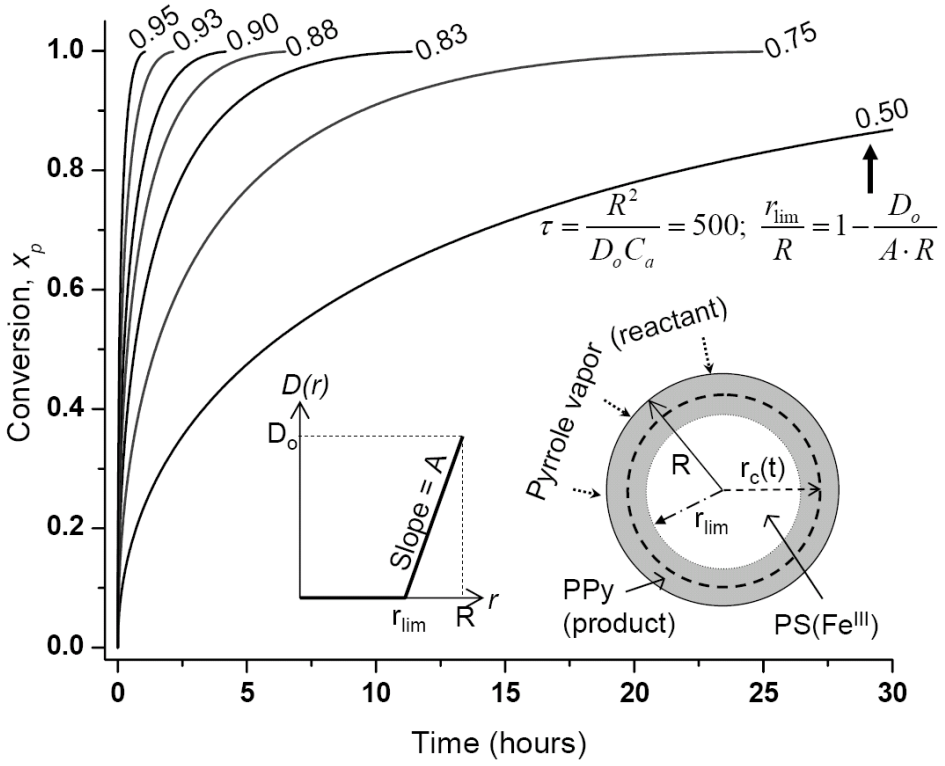

Figure S-1. Simulation of polymer growth with a cylindrical shrinking-core diffusion-reaction model assuming that the diffusion coefficient decreases linearly as the thickness of the polymer product increases. The slope A represents the dependence of diffusion coefficient, D(r), on the reaction product thickness (r). The radius $r_{lim} = R - D_o/A$ is where the diffusion coefficient becomes zero and the reaction stops. The reaction front radius is represented with $r_c(t)$. The conversion x_p is defined by the amount of PPy produced at a given time divided by the maximum amount that can be produced for the given system.

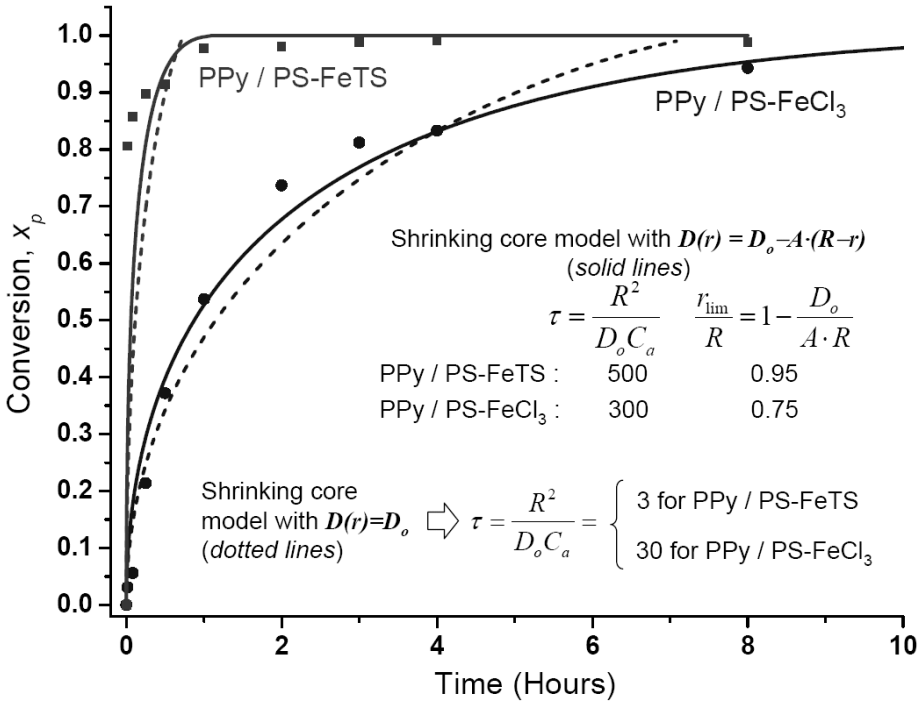

Figure S-2. Shrinking core model fit of the growth of PPy peak in FTIR. The solid lines are the fit results obtained with the cylindrical shrinking-core diffusion-reaction model for the case where the diffusion coefficient decreases as the reaction progresses. The dotted lines are the fit with the constant diffusion coefficient assumption. The conversion x_p is defined by the amount of PPy divided by the maximum amount produced.